

Research Article

# Fault Analysis of 600MW Generator Stator Bars in a Power Station

Fang Yuan\*

Datang Hydropower Science & Technology Research Institute Co., Ltd, Nanning, China

## Abstract

The stator bar, as the component connecting the coils in the generator to the external circuit, is the main carrier of current and electric field. It is hailed as the "heart" of the generator and plays a crucial role in it. Based on the specific fault phenomena of the stator bar of a 600MW large power station generator under complex operating conditions, this paper analyzes the fault causes in combination with the disassembly inspection. The direct cause of the fault is determined to be the grounding of the stator bar and the iron core. Furthermore, a three-dimensional numerical model of the stator bar is constructed based on the high-precision finite element analysis method, focusing on internal defects and their mechanism of partial discharge characteristics. It is pointed out that internal defects caused by different reasons will lead to increased partial discharge at the defects, and the main insulation will deteriorate due to the continuous influence of partial discharge during operation. The research and analysis results can provide a reference for the operation, maintenance, and fault diagnosis of the same type of stator bars to a certain extent, and have positive significance for promoting the continuous optimization, improvement, and professional management of the same type of equipment.

## Keywords

Stator Bar, Air Gap Defect, Failure Analysis

## 1. Introduction

In modern power systems where renewable energy sources are increasingly important, hydro-generators, as one of the core equipment in hydropower stations, have their operational stability and reliability directly related to the power generation efficiency and economic benefits of these stations. With the continuous growth in power demand, the unit capacity of large hydro-generator sets has been continuously increased, placing increasingly stringent requirements on the performance and reliability of the critical internal components within these generators. Stator bars, as an important component of hydro-generators, are likened to the

"heart" of the generator, and their operational status directly determines the service life, safety, and stability of the generator [1-5].

In actual operation, stator bars are prone to failures due to the combined effects of electromagnetic forces, mechanical stresses, thermal stresses, and environmental factors over extended periods of operation [6-9]. Therefore, conducting in-depth research and analysis into stator bar failures is crucial for ensuring the safe and efficient operation of power systems. A method for locating single-phase ground faults in generator stator windings based on phasor analysis was proposed in

\*Corresponding author: 453350827@qq.com (Fang Yuan)

**Received:** 7 November 2024; **Accepted:** 21 December 2024; **Published:** 27 December 2024



Copyright: © The Author(s), 2024. Published by Science Publishing Group. This is an **Open Access** article, distributed under the terms of the Creative Commons Attribution 4.0 License (<http://creativecommons.org/licenses/by/4.0/>), which permits unrestricted use, distribution and reproduction in any medium, provided the original work is properly cited.

study [10], providing a reference for technicians to locate faults in the early stages of their occurrence. In study [11], a classification and analysis of the causative mechanisms of corona discharge in stator bars were conducted based on practical cases, and treatment suggestions were provided. In study [12], an analysis database was established by collecting data on stator bars, generator cores, and their vibration peaks. Technicians can then judge the fault type by comparing measured data with the contents of the analysis database. The authors in [13] established several stator bar models with different defect types, identified partial discharge signals with different defect types based on random forest method, and compared with traditional backpropagation neural network method, proved that the recognition accuracy was improved. Phase amplitude characteristic maps for three common types of stator bar surface discharges were extracted in study [14], and comparisons with real-world cases on the worksite demonstrated the high accuracy of these maps.

This paper is based on specific fault phenomena observed in stator bars of a 600MW generator operating under complex conditions. It employs high-precision finite element analysis to construct a three-dimensional numerical model, focusing on internal defects and their mechanisms related to partial discharge characteristics. Finally, corresponding preventive suggestions are proposed for such fault issues. The research analysis results can provide references for the operational maintenance and fault diagnosis of similar stator bars to a certain extent, and have positive implications for promoting the continuous optimization, improvement, and professional management of similar equipment.

## 2. Incident Situation

The manufacturer of the generator for Unit 5 at a certain power station is Toshiba Hydro Power Equipment (Hangzhou) Co., Ltd. The generator model is SF600-66/17150, and it was commissioned for power generation on May 27, 2016. It has a rated capacity of 666,670 kVA, a rated power factor of 0.9 (lagging), a rated voltage of 20,000 V, and a rated current of 19,246 A. The stator winding is a 3-phase, 6-branch Y-connection with 35 slots per branch, totaling 630 slots.

At 00:56:16 on June 13, 2024, while Unit 5 generator at the power station was operating with a load of 600 MW, the stator grounding protection of both Sets A and B of the generator protection activated, followed by the shutdown and decoupling of the generator. Based on the comprehensive analysis of the protective action report and fault waveform recording, it is determined that a single-phase ground fault occurred in the unit, with Phase A being the faulted phase.

## 3. Disassembly Inspection and Analysis

### 3.1. Check the Condition Around the Stator Bar

After searching and confirmation, the faulty stator bar was

identified as the upper-layer bar in slot 331. Inspection revealed that there was obvious carbonized material adhering near the tooth pressure plate on this upper-layer stator bar, as shown in Figure 1. This adherent material should have been produced during the discharge of the faulty stator bar. Additionally, no abnormalities such as foreign objects, contamination, or loosening of the slot wedge were found on or around the stator bar.

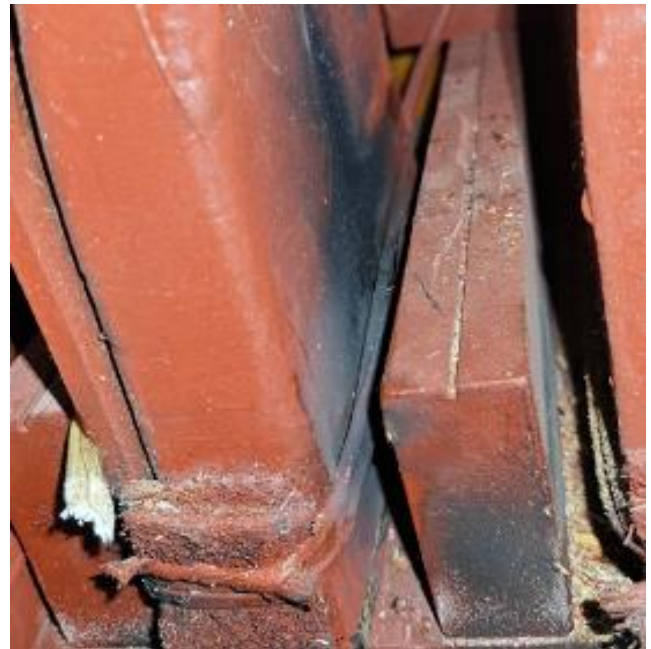


Figure 1. Carbonized material attachment.

### 3.2. Inspection of Stator Bar Body

To further investigate the cause of this fault, the faulty stator bar was lifted out for inspection, and two major abnormalities were found: First, there was a noticeable discharge ablation and carbonization point on the interlayer side of the stator bar. The main characteristics of this discharge point were as follows: It was located approximately 20mm from the slot outlet on the interlayer side of the stator bar and about 180mm from the upper end of the straight segment of the stator bar. The discharge point was approximately a 10mm diameter circular pit, exhibiting a typical concave hollow morphology overall. Second, there was a hollow and loose air gap at the edge of the discharge point on the stator bar, accompanied by a circular arc-shaped pit with a length of about 5mm and a depth of about 0.8mm. This pit was likely caused by factors such as compression, while the hollow and loose air gap was believed to have been formed when the insulation layer of the stator bar expanded due to heat during the fault, allowing air to enter and causing the hollow and loose condition, as shown in detail in Figures 2 and 3.



Figure 2. Breakdown point of stator bar.

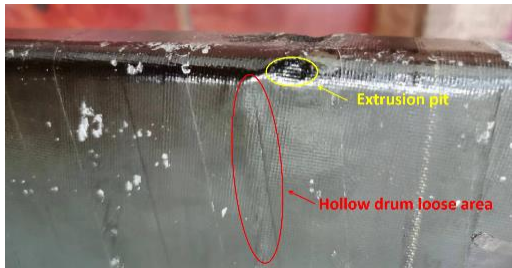


Figure 3. Hollow drums and pits at the edges of stator bar.

### 3.3. Temperature Pad Strip Inspection

During the inspection of the slot, it was found that the temperature measurement pad corresponding to the discharge area of the stator bar had a certain degree of burnout and carbonization. As shown in Figure 4, after removing the temperature measurement pad, it was observed that the underlying stator bar was free of any abnormalities. Upon layer-by-layer stripping of the temperature measurement pad, it was found that the carbonization point did not penetrate through, and the lead-out wire and potting of the pad were intact and without damage. Therefore, it could be ruled out that the stator bar fault was caused by overheating due to a short circuit in the temperature measurement pad. Combining the inspection results, it can be concluded that the discharge point was caused by discharge breakdown originating from internal factors within the stator bar.



Figure 4. Location of the burning point of the side temperature measuring pad between layers.

### 3.4. Disassembly and Inspection

The faulty upper stator bar in slot 331 and a spare stator bar from the same batch were sent back to the manufacturer for disassembly, analysis, and inspection.

#### 3.4.1. External Inspection

The dimensions of the two stator bars were measured, with widths ranging from 26.7 to 27.9 mm and heights from 80.9 to 81.4 mm. By tapping the stator bars with a small copper hammer and listening to the echo, it was determined that both stator bars had void sections within the allowable range. Radiographic inspection of the two stator bars revealed no defects such as cracks or metallic inclusions within the main insulation [15].

#### 3.4.2. Electrical Testing

The surface resistance tests of the two stator bars showed no abnormalities; the partial discharge values of both stator bars at 20 kV did not exceed 200 pC; the initial dielectric loss values were both less than 0.6%, with  $\Delta \tan \delta$  less than 0.5%; there was no corona phenomenon during the 45 kV/1 min AC withstand voltage test; in the instantaneous breakdown test, the spare stator bar did not experience creepage breakdown at 158.6 kV, while the remaining section of the repaired faulty stator bar had a breakdown voltage of 81.1 kV, as shown in Figure 5.



Figure 5. Stator bar transient breakdown test.

#### 3.4.3. Cross-Sectional Inspection

After removing the welding head and separating the strands of the faulty stator bar, it was found that there was a short circuit between wires number 1 and 68. After truncating the faulty section, the remaining part showed no short circuit. The short circuit was caused by the damage to the insulation between the copper tape and the conductor at the transposition point at the upper end, resulting in a short circuit between strands number 01 and 68. The short circuit was confirmed by measuring the resistance between the copper tape and the transposed strands (only 8.5Ω), which verified that there was a short circuit between the copper

tape and the transposed strands within the breakdown section. Figure 6 illustrates the truncation position of the stator

bar and the schematic diagram of the internal shielding process.

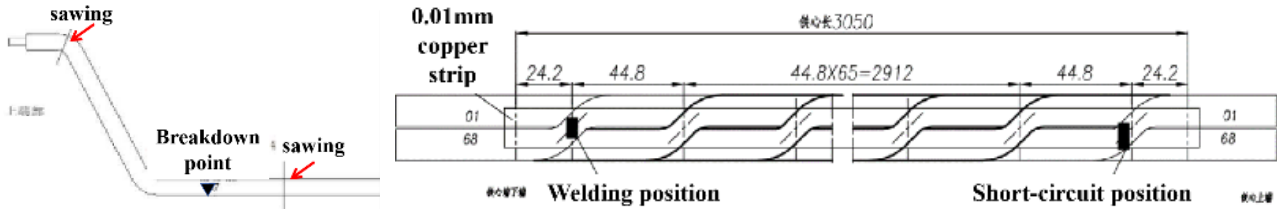


Figure 6. Internal shielding process diagram.

Mark the cut off breakdown segment bar in sections and then cut the segment as shown in Figure 7, so as to observe the wide and narrow sides of insulation and peel the insulation to observe the copper conductor surface.



Figure 7. Stator bar segment marking.

Through microscopic inspection of the cross-sections of the segment containing the breakdown point and its adjacent segments, as shown in Figure 8, the following observations can be made: The main insulation on the left side of Segment 3, which is on the same narrow surface as the breakdown point, has slight burning, but there is no insulation delamination. The main insulation on the right side of Segment 5, which is also on the same narrow surface as the breakdown point, exhibits slight delamination. On the left side of Segment 4, the insulation near the conductor surface below the breakdown point shows significant deterioration, with clear delamination of the insulation. On the right side of Segment 4, the insulation near the conductor surface below the breakdown point also shows significant deterioration, and the degree of deterioration is more severe than that on the left side. Additionally, the filling putty is overall darkened, and tiny air gaps are visible.

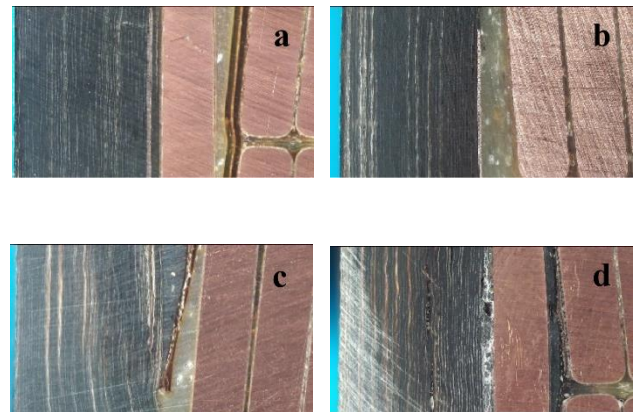


Figure 8. Microsection (a) the left of 3, (b) the right of 5, (c) the left of 4, (d) the right of 4.

After stripping the main insulation for observation, as shown in Figure 9, it was found that there were burn marks on the narrow surface of the copper conductor, which developed towards the end of the stator bar. Additionally, the hollow bulge only existed on the outer layer, and it was judged to be caused by occasional collisions and compression during the installation process, which then developed due to the insulation expanding and heating up during the fault.

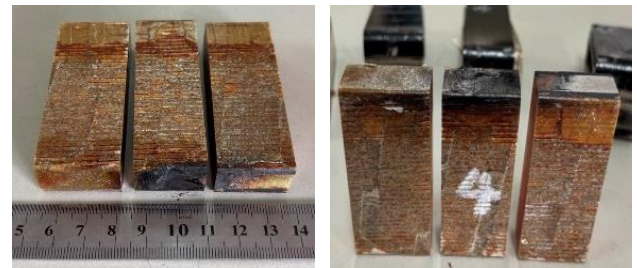


Figure 9. A copper conductor stripped of the main insulation.

### 3.4.4. Glass Transition Temperature and Density Test

Samples were taken from four locations of the faulty stator bar. Dynamic mechanical analysis (DMA) was employed to

test the insulation performance of each area of the main insulation. The test results for the linear sections are shown in Figures 10, 11.

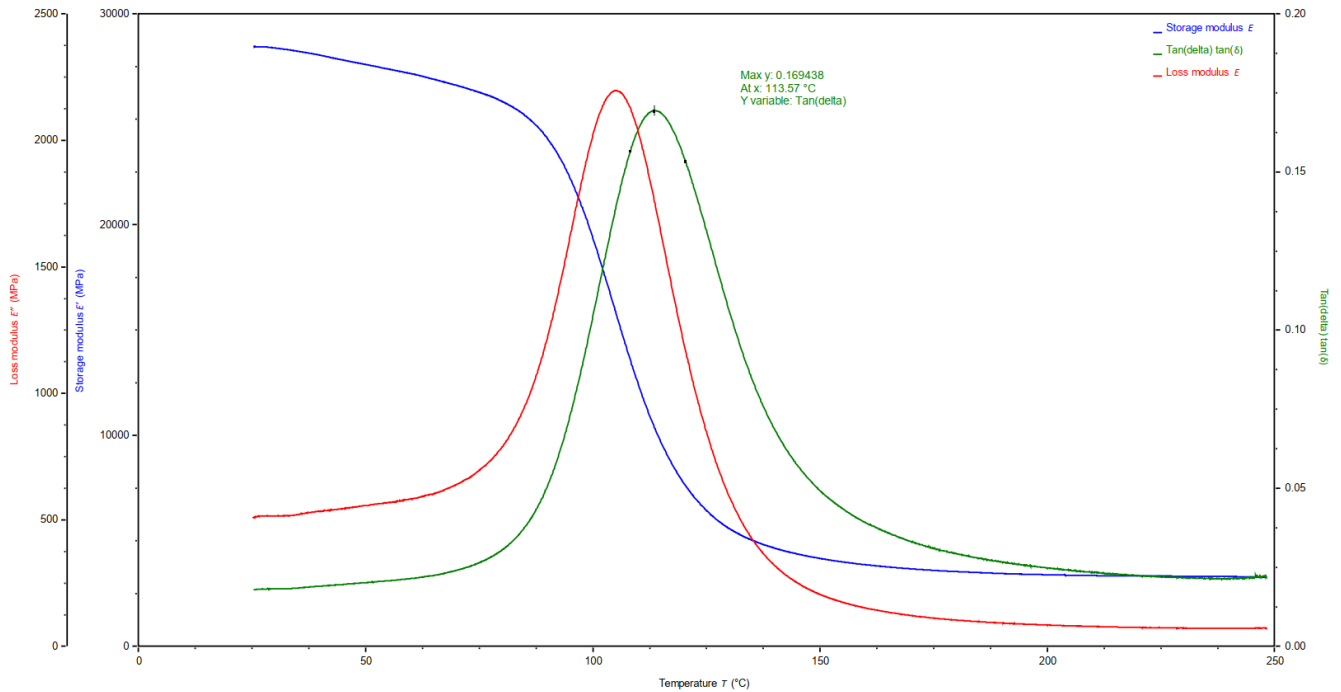


Figure 10. Sample in the middle of the linear part of the faulty stator bar (113 °C).

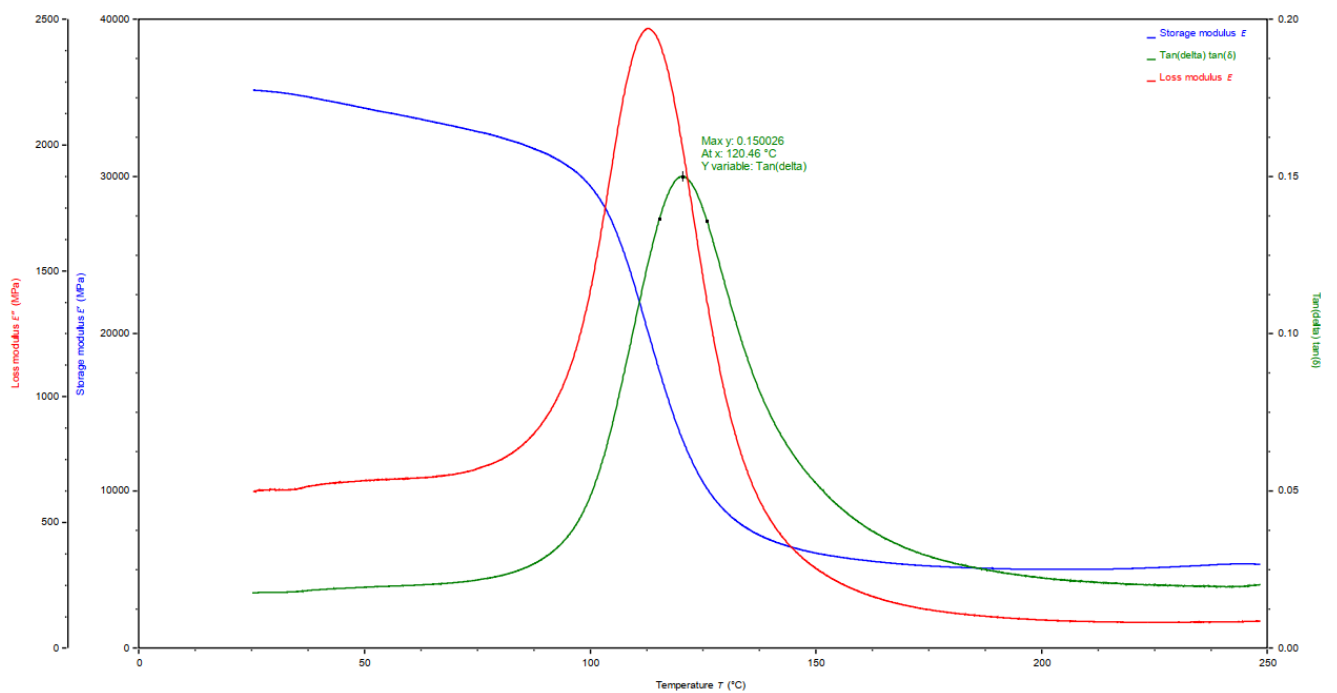


Figure 11. Sample with the linear part of the faulty stator bar near the breakdown point (120 °C).

The glass transition temperatures of the samples taken from the linear sections were similar, and the glass transition

temperatures of the samples taken from the end sections were higher than those of the linear sections. All glass transi-

tion temperatures were above 110 °C, which was comparable to the specified value of the main insulation material, indicating that there was no abnormality in the performance of the main insulation material.

After testing the glass transition temperature of the samples, their densities were also measured. The results are shown in Table 1 below:

**Table 1.** Slice density of sample.

Slice density of sample	Density (g/cm <sup>3</sup> )
Center segment of the line part	1.804495712
Near the breakdown point	1.822461892
Lower end of line bar	1.776406124
Top end of stator bar	1.776770608

The density test data reveals that the density of the main insulation in the straight section is slightly higher than that in the end sections. This is because the former has a higher content of inorganic substances, which have a higher density, and the resin content of the main insulation is slightly lower than that of the latter. The test results indicate that the densities of the main insulation in both sections are relatively consistent, with no insulation defects and stable curing process.

## 4. Cause Analysis

Based on the findings from the site inspection, relevant documentation, and test results, an analysis was conducted on the causes of the stator bar insulation failure.

Firstly, the preventive test reports, maintenance records, and operational logs for the past two years were reviewed, and no abnormalities were found in the test data. Prior to the failure, the temperature of the temperature measurement pad in the slot was approximately 80 °C, which was basically consistent with the operating temperatures of other stator bars. This temperature was far below the maximum allowable long-term operating temperature of 155 °C for Class F insulated stator bars. Therefore, insulation aging due to overheating of the stator bar could be ruled out.

Secondly, no whitening of the insulation material surface due to long-term corona discharge was observed at the discharge point and its surrounding area on the faulty stator bar. The low-resistance tape wrapping the discharge breakdown point was intact. Combined with the design dimensions of the high- and low-resistance tapes on the stator bar, corona discharge caused by improper transition between the high- and low-resistance tapes could be eliminated.

Thirdly, the possibility of stator bar foreign matter defects was considered. When magnetic metal substances are present inside the stator bar, it can lead to heating, vibration, and partial discharge, gradually deteriorating the insulation material and ultimately causing stator bar failure. Considering the increasingly improved industrial manufacturing environment, the possibility of metal contamination is low, but cannot be completely ruled out.

Lastly, the possibility of damage during the installation process of the stator bar was considered. Pre- and post-installation inspections and test results were all qualified and showed no abnormalities. However, due to uncontrollable factors such as personnel skill levels during the installation process, it is inevitable that some parts of the stator bar may suffer from collisions and compressions during the wiring and transportation stages. The collided and compressed areas may experience reduced insulation strength or slight insulation delamination. Nevertheless, after installation, the stator bar still maintained a certain level of insulation strength, sufficient to withstand both test and operating voltages, making it difficult to detect insulation issues in these areas during maintenance tests. However, the presence of insulation delamination in these areas created air gaps, which led to partial discharges and gradually eroded the insulation.

## 5. Electric Field Simulation Calculation

In order to verify the effect of air bubbles or metal impurity defects on the electric field distribution in the main insulation, the following simulations were carried out in COMSOL Multiphysics.

### 5.1. Simulation of Effect of Air Gap on Electric Field Distribution

Using the corresponding dimensional data and material design values of the faulty stator bar, a three-dimensional simulation model was established, as shown in Figure 12. By setting the potential of the copper conductor to 20kV and grounding the outer edge of the main insulation, the operating conditions were simulated. A tiny bubble with a radius of 0.1mm was introduced within the narrow-side main insulation layer to mimic the air gap defects that may arise after compression. The resulting electric field intensity distribution from the simulation is presented in Figure 13. It can be seen from the figure that the presence of the bubble leads to distortion in the electric field intensity, with the highest field intensity at its boundary reaching  $1.4 \times 10^6$  V/m. Clearly, when bubbles defects exist in the main insulation, they will inevitably cause excessively high local field intensities under the action of operating voltages, leading to partial discharges and subsequent insulation degradation.

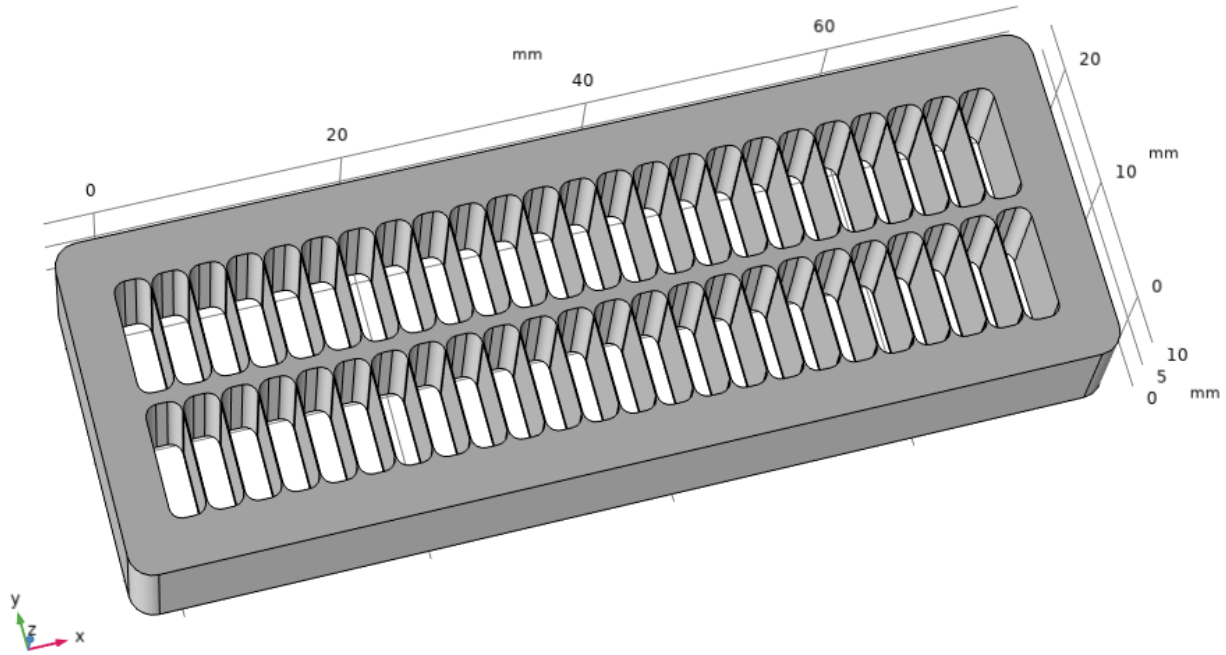


Figure 12. 3D model.

insulation layer on the narrow side of the stator bar, thus deteriorating the overall electric field environment. If non-conducting materials are also mixed in, the risk of partial discharge is high.

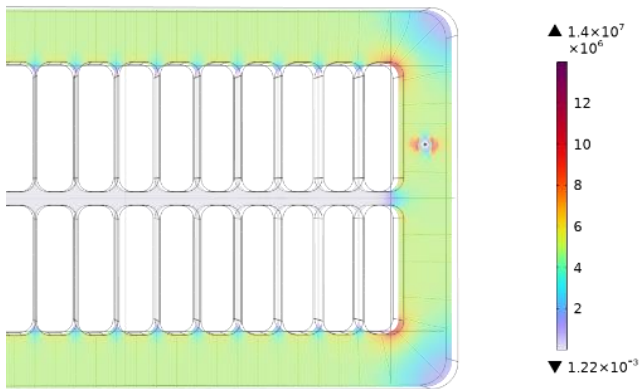
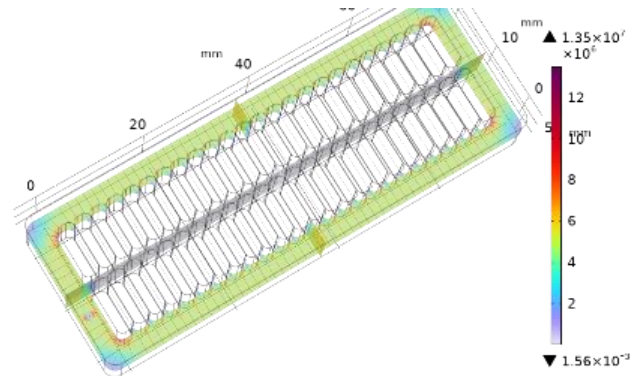


Figure 13. Main insulation electric field distribution with bubble defect.



### 5.2. Simulation of the Influence of Metal Impurities on Electric Field Distribution

By setting a copper particle with a radius of 0.1mm in the main insulation to simulate metal impurities entering during the production process, with other parameter settings the same as in Section 4.1. When metal impurities are mixed into the main insulation material due to production processes, the corresponding electric field distribution is shown in Figure 14. At this time, the maximum electric field intensity is  $1.35 \times 10^7$  V/m, and the metal impurities are at a floating potential in the main insulation material. Similar to the bubble defect, the presence of metal particles leads to an expansion of the high electric field intensity area in the main insulation, and the area of electric field distortion almost spans the main

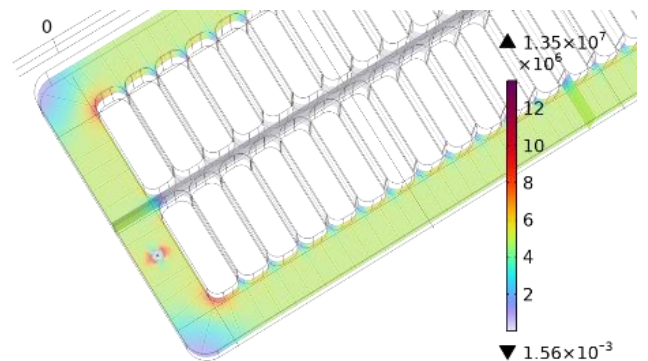


Figure 14. Distortion of electric field distribution caused by metal defects.

## 6. Conclusions

This paper studied and analyzed the stator bar fault of a 600MW generator in a power station. By analyzing the evolution process of the fault and the on-site disassembly, the fault eliminated the external factors such as pollution accumulation, temperature measuring pad strip, slot wedge loosening, batch manufacturing defects and the possibility of overheating of the stator bar. The possible causes were bubbles and metal foreign matter defects in the main insulation of the stator bar. Based on the finite element principle, the stator bar is modeled and simulated. Through the simulation calculation, it is found that when there are bubbles or metal foreign body defects in the interior, partial discharge will occur, and finally insulation deterioration until breakdown. The analysis results can provide a reference for the operation, maintenance, and fault diagnosis of the same type of stator bars to a certain extent, and have positive significance for promoting the continuous optimization, improvement, and professional management of the same type of equipment.

Further work can be done by analyzing the characteristic data of the generator partial discharge online monitoring system, establishing a comparative database, and analyzing the influence of various fault types on the deterioration trend of the stator bar, which can guide the relevant technicians to identify the characteristics in the early stage of the fault and confirm the type after the fault occurs.

## Abbreviations

DMA Dynamic Mechanical Analysis

## Author Contributions

Fang Yuan is the sole author. The author read and approved the final manuscript.

## Conflicts of Interest

The authors declare no conflicts of interest.

## References

- [1] Ge Chenzhong, Ning Suhui, Fu Qiang, et al. Impact Factors on Large Generator Stator Windings Insulation Property. *Large Electric Machine and Hydraulic Turbine*, 2014, (3): 35-40. <https://doi.org/10.3969/j.issn.1000-3983.2014.03.011>
- [2] Liu Xiangdong, Xiao Fafu, Huang Minghao, et al. Insulation Breakdown Fault Analysis of Stator Bar for Pumped Storage Generator. *Water Resources and Power*, 2020, 38(12): 145-148, 175.
- [3] Han Lin, Pan Zhongping. Diagnosis and Countermeasures of Stator Winding Faults of Hydro-generators. *Large Electric Machine and Hydraulic Turbine*, 2021, (6): 44-46, 74. <https://doi.org/10.3969/j.issn.1000-3983.2021.06.008>
- [4] Gao Zongbao, Wu Guangning, Jiang Jian ming, et al. Analysis and Research on Stator Earthing Fault of Large Hydro-generator Set, *Electrotechnical Application*, 2017, 36(23): 46-50.
- [5] Ning Guoxing. Cause Analysis and Prevention of Stator Rotor Insulation Failure of Hydrogenerator. *China Water Resources*, 2012, (12): 33-34. <https://doi.org/10.3969/j.issn.1000-1123.2012.12.015>
- [6] Tan Liming, Yin Xianggen, Wang Yikai, et al. An Adaptive Load-Based Location Method of Stator Ground Fault for Large Hydro-Generators, *Transactions of China Electrotechnical Society*, 2022, 37(17): 4411- 4422. <https://doi.org/10.19595/j.cnki.1000-6753.tces.211155>
- [7] Qiao Jian, Yin Xianggen, Wang Yikai, et al. Slot potential based stator grounding fault location method for large generator. *Electric Power Automation Equipment*, 2022, 42(11): 204-210, 217. <https://doi.org/10.16081/j.epae.202204003>
- [8] Pan Jiannan, Li Haoliang. Analysis of Insulation Breakdown Caused by Interlayer Strip Defect of Generator Stator Bar. *Large Electric Machine and Hydraulic Turbine*. 2022, (06): 43-47+54. <https://doi.org/10.3969/j.issn.1000-3983.2022.06.008>
- [9] Chen Junwei, Li Jianfa. Analysis on the Cause of Short Circuit Fault in Generator Stator Winding. *Electric Engineering*. 2018, (13): 78-79. <https://doi.org/10.3969/j.issn.1002-1388.2018.13.026>
- [10] Hou Xiaohu, Zhang Ke, Gong Linping. A new method of generator stator grounding fault location based on phasor analysis. *Mechanical & Electrical Technique of Hydropower Station*. 2021, 44(11): 4-7. <https://doi.org/10.13599/j.cnki.11-5130.2021.11.002>
- [11] Han Jianbo, Wang Jisheng, Wang Xiaoyu. Analysis and treatment of stator rod corona of large pump motor. *Mechanical & Electrical Technique of Hydropower Station*. 2023, 46(01): 55-57. <https://doi.org/10.13599/j.cnki.11-5130.2023.01.017>
- [12] Zhang Hong, Wu Mingbo, Zhang Xingming, et al. An Insulation Fault Detection Method of Generator Stator Core Based on Data Analysis. *Hydropower and Pumped Storage*. 2022, 8(3): 78-80. <https://doi.org/10.3969/j.issn.2096-093X.2022.03.016>
- [13] Hu Jianglin, Zhang Xi, Song Zhan, et al. Recognition Method of Partial Discharge Spectrum Feature in Generator Stator Bar Based on Random Forest. *High Voltage Engineering*. 2024, 50(3): 1272-1280. <https://doi.org/10.13336/j.1003-6520.hve.20230218>
- [14] Li Hongfei, Gao Zongbao, Cai Youwei, et al. Analysis of discharge faults in stator windings of simulated large hydroelectric generators and its application simulation research on real wire rod model. *Electric Power Technology and Environmental Protection*. 2023, 39(3): 207-214. <https://doi.org/10.19944/j.eptep.1674-8069.2023.03.004>
- [15] Liu Ling, Zhang Yu, Jin Dongsong, et al. Mechanism of Insulation Deterioration of Large Generator Stator Bars Eroded by Metal Impurities. 2022, 56(6): 104-111, 194. <https://doi.org/10.7652/xjtuxb202206013>

## Biography



**Fang Yuan** is a senior engineer at China Datang Hydropower Science and Technology Research Institute. He has 20 years of working experience. He holds bachelor's and Master's degrees in electrical engineering. His area of interest is equipment failure analysis.

## Research Field

**Fang Yuan:** Analysis of generator stator fault., Stator bar repair, Lightning protection for transmission lines, High voltage and insulation technology, Fault diagnosis and analysis of casing.